JACS
JOURNAL OF THE AMERICAN CHEMICAL SOCIETY

ARTICLE

pubs.acs.org/JACS

Acidification of Reverse Micellar Nanodroplets by Atmospheric Pressure CO_2

Nancy E. Levinger,* Lauren C. Rubenstrunk, Bharat Baruah,† and Debbie C. Crans*

Department of Chemistry, Colorado State University, Fort Collins, Colorado 80523-1872, United States

Supporting Information

ABSTRACT: Water absorption of atmospheric carbon dioxide lowers the solution pH due to carbonic acid formation. Bulk water acidification by CO_2 is well documented, but significantly less is known about its effect on water in confined spaces. Considering its prominence as a greenhouse gas, the importance of aerosols in acid rain, and CO_2-buffering in cellular systems, surprisingly little information exists about the absorption of CO_2 by nanosized water droplets. The fundamental interactions of CO_2 with water, particularly in nanosized structures, may influence a wide range of processes in our technological society. Here results from experiments investigating the uptake of gaseous CO_2 by water pools in reverse micelles are presented. Despite the small number of water molecules in each droplet, changes in vanadium probes within the water pools, measured using vanadium-51 NMR spectroscopy, indicate a significant drop in pH after CO_2 introduction. Collectively, the pH-dependent vanadium probes show CO_2 dissolves in the nanowater droplets, causing the reverse micelle acidity to increase.

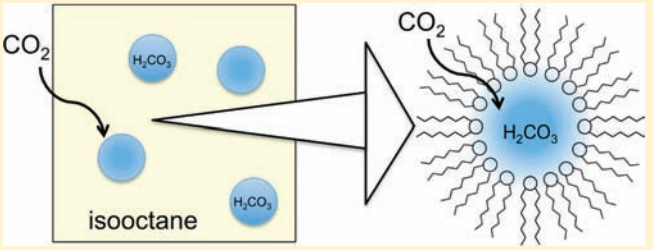

I. INTRODUCTION

Carbon dioxide has environmental impact through its effects as a greenhouse gas,[1] its ability to acidify the world's surface waters,[2] and its role in maintaining physiological pH.[3] These issues demand our attention, but the acidification problem often stands in the shadow of global warming. Given rising CO_2 levels in our atmosphere, it is important to develop an understanding of processes that can impact acidity in aerosols, which may ultimately affect the delicate balance in lakes, rivers, and oceans. Although CO_2 absorption and its reaction to form carbonic acid or bicarbonate have been characterized in bulk aqueous solution,[4−6] much less is known about CO_2 absorption into small water droplets, microheterogeneous media, or aerosols. Furthermore, acid/base chemistry at interfaces can diverge significantly from bulk aqueous behavior and is important for many chemical and biological processes such as cellular uptake, corrosion, ice nucleation, and cloud formation.[7,8]

One might predict that nanoscopic water pools found in many confined environments, such as reverse micelles, nanostructured materials, and cell organelles, might be sheltered from pH changes incurred by the presence of atmospheric CO_2. Given the interest in nanoscopic water and the utility of microheterogeneous environments for nanoparticle synthesis,[9] as models for biological substructures,[10] in green chemistry applications,[11] and as models for prebiotic aerosols,[12] knowing and controlling the acidity in these nanoscopic water pools is important for optimizing their use. Although absorption of gases such as OCS or SO_2 by aerosol droplets, yielding SO_4^{2-}, has been well studied, far less is known about absorption of CO_2 into aerosols. Here, we report on studies demonstrating facile absorption of CO_2 into water pools in reverse micelles, showing that CO_2 absorption leads to dramatic changes in local acidity, even though the number of water molecules in each water pool is too small to define pH.

Our experiments employ reverse micelles formed when aerosol-OT (AOT, sodium bis-2-ethylhexyl sulfosuccinate) surfactant surrounds a water pool to create nanosized water droplets in isooctane.[13] Figure 1 shows the structure of AOT and a suggested form for the reverse micelles. Particles in these dynamic suspensions have a known size defined by $w_0 = [H_2O]/[AOT]$; their spherical form leads w_0 to be directly proportional to the average reverse micelle radius.[13] Confined environments, such as those found in reverse micelles, can impact a wide range of different processes; for instance, nanoscopic environments strongly limit molecular motion.[14−21] Various properties of the intramicellar water differ significantly from those of bulk water. For example, both acidic and basic solutions used to form reverse micelles tend toward neutral pH in the interior water pool.[8,15,22−24] Likewise, interactions with the reverse micellar interface disrupt hydrogen bonding, causing impairment of water reorientation.[21,25,26] Solution properties found in microemulsions also differ from the bulk organic solvent properties.[13,27−30]

Given the nanoscopic nature of reverse micelle water pools, their acidity cannot be probed using a conventional pH meter. Researchers generally enlist molecular probes to report on the intramicellar pH.[31−38] Each molecular probe has its own limitations, such as pK_a and changes that may occur in microheterogeneous

Received: February 16, 2011
Published: April 20, 2011

dx.doi.org/10.1021/ja2011737 | J. Am. Chem. Soc. 2011, 133, 7205–7214

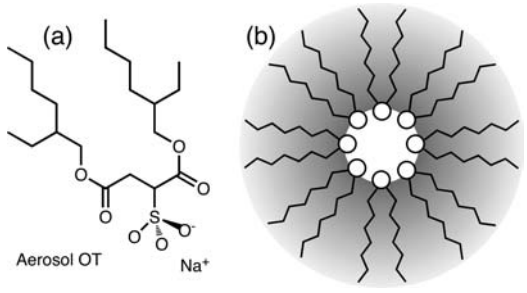

Figure 1. (a) Molecular structure of the surfactant aerosol OT (AOT) used in these studies. (b) Cartoon figure of a reverse micelle. The interior (white) represents a water pool surrounded by surfactant molecules in nonpolar solvent (gray).

environments, location of the probe in the microheterogeneous environment, and the probe effect on system (buffering, disruption, changes in microenvironment, H-bonding).[31−38] With only one acid group, probes such as acridine orange base[33,34] and bromophenol blue[39] have limited suitability for determining pH over a broad pH range. The multiple protonation states for fluorescein and its derivatives make them much more versatile, and researchers have used them to explore the acid/base characteristics of the AOT reverse micellar water pools.[32,37,38] However, significant differences in hydrophobicity of the various protonation and tautomeric states can lead the probe to reside in dramatically different locations in the reverse micelles, moving from the interior "bulk water"-like environment to the interface and potentially even embedding in the micellar interface.[32,37,38] In a recent paper, Halliday et al. reported using ^{1}H NMR relaxation measurements to follow proton changes in reverse micelles.[40] They observe changes in the T_2 time for alcohol protons in cetyltrimethylammonium bromide and Triton X-100 reverse micelles prepared with aqueous solutions of varying pH values. These studies are limited to acidic pH ranges, and because they probe OH groups on the surfactant or cosurfactant, this method only applies to the reverse micelle interface.

We have developed a method to measure apparent pH in AOT reverse micelles over an extended pH range using a class of pH-sensitive vanadium probes: i.e., oxovanadates.[15,22] The relative oligomerization and protonation states of these species, readily prepared from aqueous solutions of metavanadate (VO_3^-) (or orthovanadate, VO_4^{3-}), reflect the local pH in solution.[41−44] Because they contain vanadium, one or more signals in the ^{51}V NMR spectrum characterize the relative proportion of each vanadate oligomer and its various protonation states, which depend intimately on the pH of the system.[41,43,44] Equilibria governing the speciation in bulk aqueous solution are well-known, and speciation can be determined from the known equilibrium constants.[41−43] Importantly, ^{51}V NMR sensitively measures the relative abundance of each species, allowing determination of the reverse micelle water pool pH. We have shown oxovanadates are highly effective spectroscopic probes for monitoring apparent pH changes in the reverse micelle interiors.[15,22]

Here, we present results from experiments exposing AOT reverse micelles and aqueous samples, each containing the vanadium probes, to an atmosphere[45] of CO_2 gas sublimed from dry ice, which displaces the air above the solutions. We monitor changes in the intramicellar pH through the response of the vanadate probes.

II. MATERIALS AND METHODS

A. Materials. Sodium metavanadate, $NaVO_3$ (99.9%), purchased from Aldrich was used as received. Sodium bis(2-ethylhexyl)sulfosuccinate (AOT; ≥99%, Aldrich) was purified by dissolving in methanol and stirring overnight in the presence of activated charcoal. Subsequent filtration and removal of methanol by distillation under vacuum yielded AOT free from acid impurities that was suitable for use.[46,47] Isooctane (2,2,4-trimethylpentane, 99%, Aldrich) was evaluated for impurities[48] and used without further purification. Doubly distilled and deionized water (18 MΩ cm, Barnstead E-pure) was used throughout.

B. Vanadate Solution Preparation. Vanadate solutions were prepared by dissolution of $NaVO_3$ into doubly distilled and deionized water in a volumetric flask while heating. The vanadate stock solutions were prepared to 50.0 mM vanadium. The pH values of the aqueous vanadate solutions were measured at 25 °C using an Orion 2Star pH meter calibrated with three buffers of pH 4.01, 7.00, and 10.01. The pH of the vanadate aqueous solutions was adjusted using NaOH or HCl, to achieve the desired pH value.

C. Reverse Micelle Preparation. A 0.2 M AOT stock solution was prepared by dissolving AOT in isooctane. Aliquots of aqueous vanadate solutions at pH 6.3, 9.8, 11.8, and 12.0 were added to the AOT/isooctane stock solution to yield reverse micelles. We adjust the micelle size, w_0, defined as the molar ratio of aqueous solution to surfactant, $w_0 = [H_2O]/[AOT]$. Dynamic light scattering (DynaPro Titan, Wyatt) measurements confirmed the formation and size of the reverse micelles formed. Experiments presented in the manuscript focused on one size, $w_0 = 12$; however, other sizes were explored, including $w_0 = 8, 20$. We focused on the $w_0 = 12$ reverse micelles for several reasons. First, this size represents an intermediate regime where a significant fraction of the water interacts directly with the interface, about 36%, but a sufficient fraction of the water can still completely solvate the vanadate species and form a water pool with bulk characteristics. This amount of water is sufficient to hydrate the vanadate and form the bulk water pool in the micelles. Although the size of the water pool is significant in $w_0 = 12$, it is by no means in a range where the conventional concept of pH can be used.

D. ^{51}V NMR Spectroscopy. ^{51}V NMR spectra were recorded using two separate Varian INOVA spectrometers operating in resonance with the 51-vanadium signal at 78.9 and 131.5 MHz. ^{51}V NMR spectra acquired at 78.9 MHz used a spectral window of 83.6 kHz, a pulse angle of 60°, and an acquisition time of 0.096 s with no relaxation delay. For the ^{51}V NMR spectra collected at 131.5 MHz, a 39.2 kHz spectral window was used with a 60° pulse angle and a 0.2 s acquisition time with no relaxation delay. ^{51}V chemical shifts were referenced against an external sample of VO_4^{3-} at pH 13 with a chemical shift of 538 ppm, which in turn had been referenced against a sample of $VOCl_3$ at 0.00 ppm.

E. Reverse Micelle Characterization. Kinetic viscosity measurements were conducted using a Cannon−Fenske routine viscometer maintained in a water bath at 25 °C. Conductivity measurements were made using an Orion 2Star conductivity meter also at 25 °C calibrated with Orion 100 μS/cm conductivity standard. Conductivities and viscosities of the reverse micellar solutions appear in Table 1. Conductivities measured agree with published values.[49]

The viscosity of the suspension decreased slightly with increasing CO_2 exposure. In a comparable study, an increased pressure of CO_2 led to a decreased viscosity of a methanol system.[50] It has been reported that the viscosity correlates directly to w_0; thus, a decreased viscosity also suggests a decreased w_0.[51] For large w_0 values, $w_0 > 10$, the vanadate speciation is conserved between reverse micelle sizes.[22] Thus, a slight reduction in the size of the reverse micelles should not impact the conclusions that CO_2 is responsible for the changes seen here for $w_0 = 12$ reverse micelles.[49] Consistency among the ^{51}V NMR spectra before and after CO_2 addition demonstrates that the reverse micelles remain intact after CO_2 has been absorbed.

Table 1. Viscosity and Conductivity Measurements Conducted at 25 °C for w_0 = 12 Reverse Micelles Formed with Aqueous 50 mM Vanadate Solution[a]

sample	viscosity (centistokes)	conductivity (μS)
w_0 = 12 reverse micelle	0.885 ± 0.01	0.2
w_0 = 12 reverse micelle + CO_2	0.789 ± 0.003	0.2

[a] Samples were measured before and after exposure to CO_2 gas. Error for conductivity measurements was ≤10%.

F. Carbon Dioxide Exposure Experiment. Carbon dioxide gas was generated from dry ice placed in a 1 L Erlenmeyer single-armed flask. The flask was sealed with a stopper, and a plastic hose was connected to the arm. The solution (10 mL) being exposed was added to a two-arm 100 mL round-bottom flask with rubber septa in both arms. A needle inserted in one of the rubber septa allowed the system to equilibrate to room pressure. Various methods were used to introduce gaseous CO_2 to the solutions. For example, CO_2 was introduced through a cannula passed through the second rubber septum, keeping the tip of the needle close to the surface of the solution but not penetrating the solution surface. Carbon dioxide gas built up in the round-bottom flask displaced air previously present. The aqueous solution and the reverse micelle suspension were purged for 20 min with CO_2. We also varied the amount of solution in the round-bottom flask from 10 to 50 mL to explore the impact of solution volume on the results. Finally, we have changed the exposure time to CO_2 to determine the approximate amount of time the reaction requires.

III. RESULTS

We have chosen several different initial pH values for solutions from which reverse micelles were formed to demonstrate pH changes upon CO_2 absorption. The different initial pH values show varying changes in vanadate speciation that clearly demonstrate pH changes produced by the absorption of CO_2 gas by the solutions. It is convenient to observe the species using ^{51}V NMR spectroscopy, because the chemical shifts of these species are sensitive to oxovanadate nuclearity and protonation state. Hence, pH changes occurring upon CO_2(g) absorption are readily monitored by the associated speciation change.

Figure 2 shows ^{51}V NMR spectra obtained for reverse micelle samples (stock solution pH 11.8, w_0 = 12) before and after exposure to CO_2, as well as bulk aqueous solutions (starting pH 11.8), for comparison. Deprotonated monomer (V_1) and dimer (V_2) dominate the vanadate species at pH 11.8;[41−44] this is reflected in ^{51}V NMR spectra of initial samples prior to CO_2 introduction shown in Figures 2a,b. Our previous work showed that the reverse micellar nanoenvironment can lead to ^{51}V NMR spectra of oxovanadates in reverse micelles to differ from their spectra in aqueous solutions from which they were formed.[22] This is evident in Figure 2b, where even though the overall vanadate concentration remains constant, the relative V_2 abundance is larger in the reverse micelle spectrum compared to the bulk aqueous solution and the peak has changed, reflecting the protonation (Figure 2a). Upon exposure to an atmosphere of CO_2 (Figure 2c,d), the ^{51}V NMR spectra change dramatically; these changes, that is, deprotonated V_1 and V_2 in the initial solutions converting into other species (mainly tetramer, V_4, and pentamer, V_5) after CO_2 exposure, reflect the acidification of water by CO_2 absorption, as summarized in eq 1. Using the known pH-dependent distribution of oxovanadate species,[41,43,44] the changes in the ^{51}V NMR spectra indicate that the pH of the

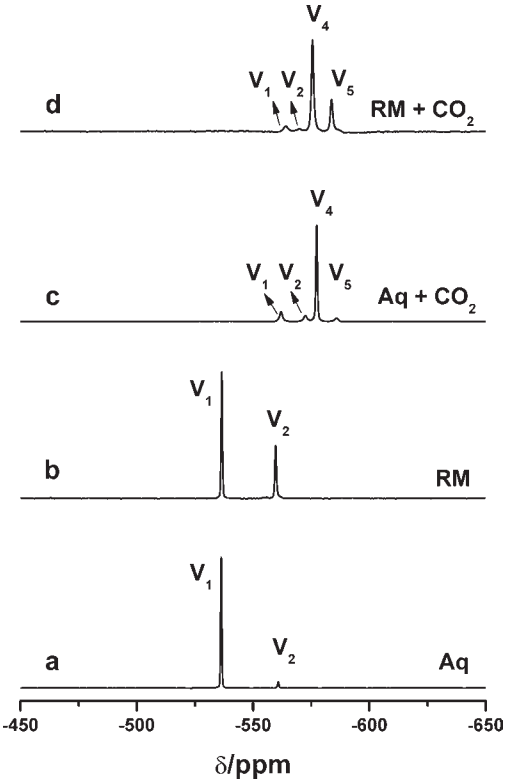

Figure 2. ^{51}V NMR spectra of vanadate in aqueous and reverse micelle samples collected at 131.5 MHz: (a) bulk aqueous vanadate solution (50 mM) prepared to pH 11.8; (b) w_0 = 12 AOT/isooctane reverse micelle suspension prepared with pH 11.8 aqueous vanadate (50 mM); (c) solution shown in (a) exposed to 1 atm of CO_2 gas for 20 min; (d) w_0 = 12 reverse micelle solution shown in (b) exposed to CO_2 gas for 20 min.

aqueous solution drops from 11.8 to 6.6 after a 20 min exposure to CO_2 at ambient temperature and pressure; the final value in the bulk aqueous solution was confirmed by measurement with a pH meter. The shift in speciation for the reverse micelle samples (Figure 2d) indicates similar acidification of the water pool to pH 6.5 to 7.

$$H_2O(l) + CO_2(g) \overset{K_1}{\rightleftharpoons} H_2O(l) + CO_2(aq) \overset{K_2}{\rightleftharpoons} H_2CO_3(aq) \overset{K_a}{\rightleftharpoons} H^+(aq) + HCO_3^-(aq) \quad (1)$$

To confirm the generality of CO_2 absorption by the reverse micelles, we conducted experiments similar to those shown in Figure 2, varying the pH of the starting probe solution and reverse micelle size (w_0), and experiments probing whether order of CO_2 addition to samples matters. Figure 3 displays the impact of CO_2 exposure on bulk aqueous solutions and reverse micelles formed with those solutions with pH 9.8 and 6.3. We chose these initial pH values because, upon acidification, the vanadate speciation displays clear changes that could be observed with ^{51}V NMR. At pH 9.8, the V_1 signal dominates the ^{51}V NMR spectrum of the bulk aqueous solution (Figure 3a) but some V_2, V_4, and V_5 also appear. The spectrum of the starting solution in w_0 = 12 reverse micelles (Figure 3b) reveals broader peaks with highest intensity in the V_1 peak, decreasing to V_2, V_4, and V_5. However, following exposure to CO_2 (Figure 3c,d),

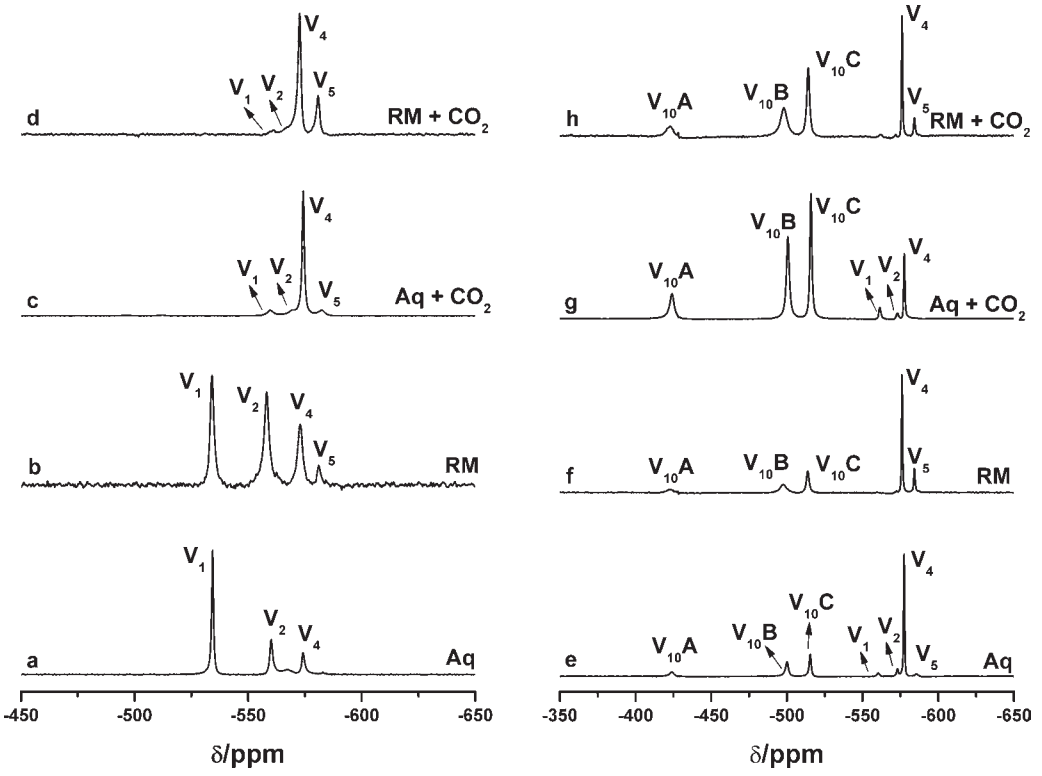

Figure 3. ^{51}V NMR spectra of vanadate in aqueous and reverse micelle samples. The left side gives spectra collected at 78.9 MHz: (a) bulk aqueous vanadate solution (50 mM) prepared to pH 9.8; (b) w_0 = 12 AOT/isooctane reverse micelle suspension prepared with pH 9.8 aqueous vanadate (50 mM); (c) solution shown in a) exposed to CO_2; (d) solution shown in (b) exposed to CO_2. The right side gives spectra collected at 131.5 MHz: (e) bulk aqueous vanadate solution (50 mM) prepared to pH 6.3; (f) w_0 = 12 AOT/isooctane reverse micelle suspension prepared with pH 6.3 aqueous vanadate (50 mM); (g) solution shown in (e) exposed to CO_2; (h) solution shown in (f) exposed to CO_2.

spectra appear to reach pH values comparable to those seen in Figure 2c,d: that is, pH 6.5−7.

The spectra for solutions starting at slightly acidic pH, 6.3 (Figure 3e−h), differ from those for basic solutions. In addition to a strong signal from V_4, three peaks characteristic for decavanadate, V_{10}, appear in both starting solutions and those exposed to CO_2. The growth of V_{10} signals shows that CO_2 causes acidic solutions to become mildly more acidic in both aqueous and reverse micellar samples. The pH value of the aqueous solution was 5.8. The similarity between the ^{51}V NMR spectra in Figure 3g,h demonstrates that the intramicellar pH is similar to that measured in the bulk aqueous sample.

Exposure of both smaller and larger reverse micelles, shown in Figure 4, yield experimentally indistinguishable ^{51}V NMR spectra, demonstrating that the overall water concentration and amount of water present per micelle has little to no impact on the final pH achieved by CO_2 exposure.

If the nature of the CO_2 interaction with the intramicellar water pool differs dramatically from its interaction with bulk aqueous solution, then we expect to observe differences depending on sample preparation. Thus, we explored whether exposing CO_2 to the stock solution prior to reverse micelle formation generated results different from those on exposing the reverse micelle samples directly. Figure 5 displays a series of ^{51}V NMR spectra for aqueous vanadate samples and reverse micelles prepared at pH 12.0 where we vary CO_2 exposure: that is, we compare reverse micelles prepared with aqueous solution that has already been exposed to CO_2 to reverse micelles exposed to CO_2 after their formation. The ^{51}V NMR spectra of vanadates in the reverse micelles treated with CO_2 show experimentally indistinguishable acidification to the stock solution treated with CO_2 and used to form the reverse micelles (Figure 5d,e). Although data in Figure 5 show only one representative pH value, additional measurements confirmed that the order of exposure to CO_2 had little impact on the resulting acidification. Furthermore, CO_2 exposure of bulk aqueous solution yielded the same final pH value regardless of the presence of vanadate in solution.

To understand the acidification of the reverse micelles, we have also performed experiments exploring the change in reaction progress as a function of time (Figure 6). By removing aliquots of the solution exposed to CO_2 gas periodically over time, we monitored the reaction to learn the extent of the reaction and to assess when CO_2 saturation was achieved. Figure 6 shows ^{51}V NMR spectra collected at 5 min intervals after starting CO_2 exposure for both samples containing AOT reverse micelles in isooctane, w_0 = 12. These spectra clearly demonstrate that the acidification reaction occurs more quickly in the reverse micellar solutions than it does in bulk aqueous solution.

IV. DISCUSSION

A. pH Changes in Reverse Micelles Resulting from CO_2 Absorption. Changes in oxovanadate speciation and protonation from our experiments demonstrate that the pH inside the reverse micelles changes when the reverse micelles are exposed to CO_2 gas. To observe probe changes associated with the drop

dx.doi.org/10.1021/ja2011737 |J. Am. Chem. Soc. 2011, 133, 7205–7214

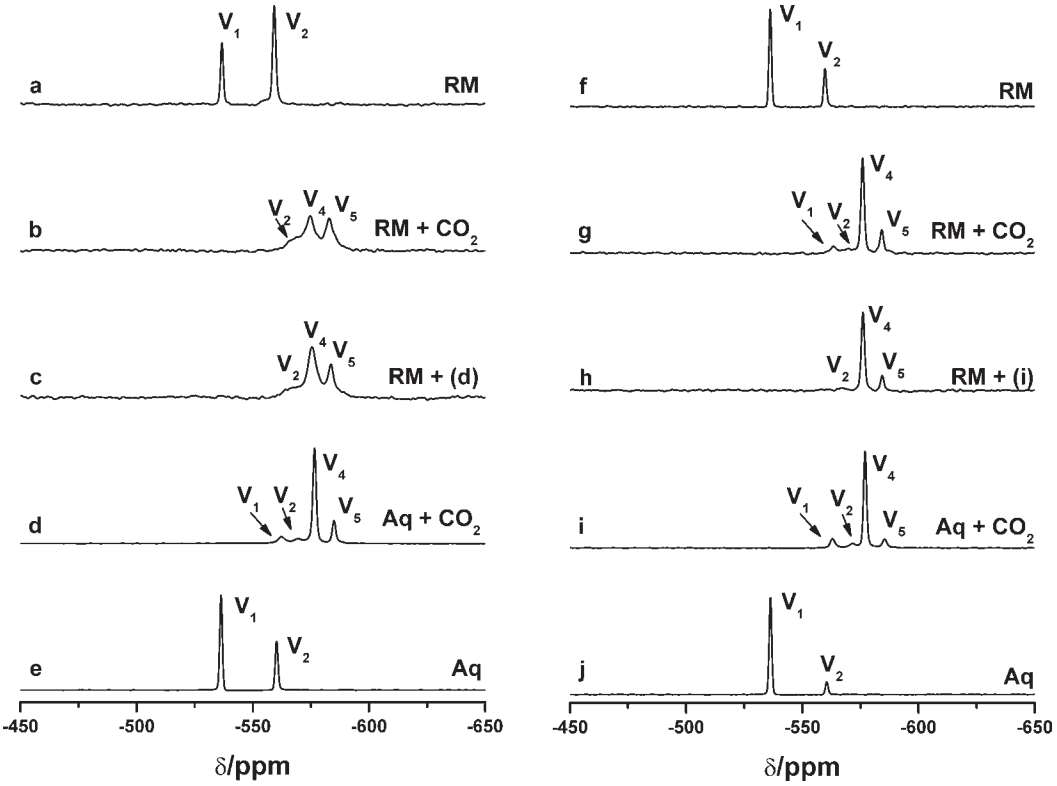

Figure 4. ^{51}V NMR spectra at 78.9 MHz of reverse micelle samples in isooctane and aqueous solutions from which samples were formed. The left side gives the following spectra: (a) w_0 = 8 AOT reverse micelles formed from solution in (e) before exposure to CO_2 gas; (b) w_0 = 8 AOT reverse micelles formed from solution in (e) after equilibration to 1 atm CO_2 gas; (c) w_0 = 8 AOT reverse micelles formed from solution in (d); (d) 50 mM aqueous vanadate solution prepared to pH 12.24 after equilibration to 1 atm CO_2 gas; (e) 50 mM aqueous vanadate solution prepared to pH 12.24 prior to exposure to CO_2 gas. The right side gives the following spectra: (f) w_0 = 20 AOT reverse micelles formed from solution in (j) before exposure to CO_2 gas; (g) w_0 = 8 AOT reverse micelles formed from solution in (j) after equilibration to 1 atm CO_2 gas; (h) w_0 = 20 AOT reverse micelles formed from solution in (i); (d) 50 mM aqueous vanadate solution prepared to pH 12.04 after equilibration to 1 atm CO_2 gas; (j) 50 mM aqueous vanadate prepared to pH 12.04 before exposure to CO_2 gas.

from pH 11.8 to 6.5−7 the proton addition resulting from absorption of CO_2 gas requires the conversion of the vanadium probe into oxovanadates found at lower pH values.[41] We calculate the average amount of CO_2 absorbed by each reverse micelle nanowater pool by considering the aqueous vanadate speciation chemistry as well as the apparent pH drop as measured by changes in ^{51}V NMR signal positions.

The details of the average amount of CO_2 absorbed by each reverse micelle nanowater pool calculation are described in the Supporting Information. Specifically, combining information about the reactions that occur to form the various vanadium compounds summarized in Scheme 1, using the relative amount of each probe present in the solution and the overall concentrations of vanadium and surfactant, we calculate the number of protons generated per reverse micelle upon exposure to the CO_2 gas. We know the overall concentrations of vanadate and surfactant and the aggregation number n_{agg} for a w_0 = 12 reverse micelle.[24] The integrated intensities of signals in the ^{51}V NMR spectra yield relative populations for each vanadium species, e.g., V_1, V_2, V_4, V_5, and V_{10}. Reactions converting the species in the starting aqueous stock solution to the species observed following CO_2 exposure (Scheme 1) approximate the number of protons required to form each species. Totaling the number of vanadium molecules of each species times the number of protons required to produce the species observed at pH 6.5 plus the protons required to effect the measured pH drop yields the total number of protons introduced. The total number of protons divided by the total number of reverse micelles yields protons per reverse micelle generated by CO_2 absorption. We find that each reverse micelle absorbs enough CO_2 to introduce, on average, an additional 1.5−2 protons to the water pool containing the vanadium probe. For pH 11.8, most of these protons are associated with the vanadate chemistry but the remaining 0.15−0.2 proton/water pool represent the pH drop in water. These calculations were performed for w_0 = 12. However, studies with other reverse micelle sizes, e.g., w_0 = 8 and 20, reveal comparable speciation changes (Figure 4).

Researchers have explored the exposure of reverse micelles to CO_2 under extreme conditions: that is, to high-pressure CO_2 (≥25 atm) and in supercritical CO_2.[23,52−56] In both these environments, results showed that the interior pH dropped from neutral to acidic pH.[23,52−54] For AOT/isooctane exposed to high-pressure CO_2,[54] experiments showed that, upon identical CO_2 exposure, the bulk aqueous solution became more acidic than the reverse micelles did, suggesting that the reverse micelles may present a barrier to CO_2 absorption. When introduced at high pressure, researchers suggest that CO_2 stabilizes the reverse micelles by adding to the interfacial layer.[28,55] However, the high pressure and supercritical CO_2 conditions used in these studies diverge far from normal atmospheric CO_2, the pressure explored in the study reported here, where we observe acidification of reverse micelle water pools. Extrapolation from high-pressure

dx.doi.org/10.1021/ja2011737 |J. Am. Chem. Soc. 2011, 133, 7205–7214

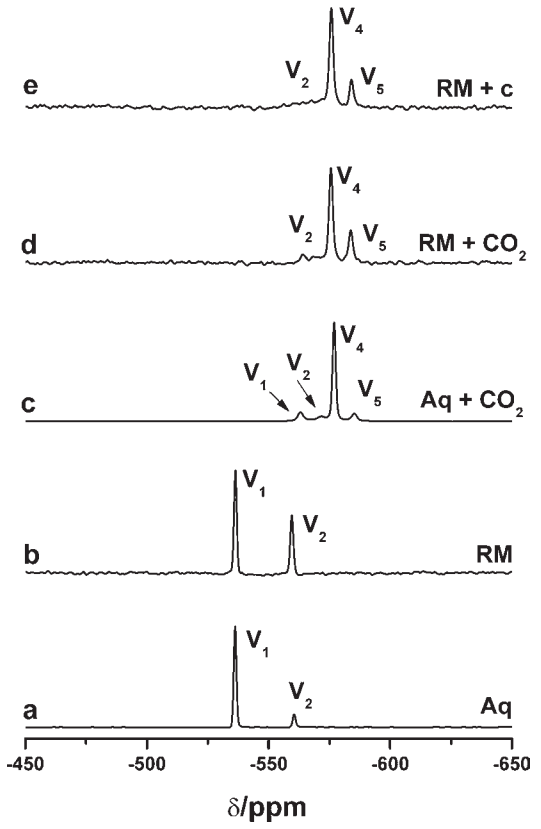

Figure 5. ^{51}V NMR spectra for aqueous and reverse micelle samples as a function of sample preparation: (a) bulk aqueous vanadate solution (50 mM) prepared to 12.0; (b) w_0 = 12 reverse micelle suspension prepared with pH 12.0 aqueous vanadate solution; (c) solution shown in a) exposed to 1 atm of CO_2 gas; (d) w_0 = 12 reverse micelle solution shown in (b) exposed to 1 atm of CO_2 gas; (e) w_0 = 12 RM suspension prepared from the aqueous sample in part (c) already exposed to CO_2. Spectra were obtained at 78.9 MHz.

studies[28,29] suggests that CO_2 should be only sparingly soluble in isooctane at atmospheric pressure. However, data in the literature report significant absorption of CO_2 gas by alkane solvents such as *n*-octane and *n*-decane.[57] We have observed the same results for isooctane when our AOT reverse micelle samples were degassed prior to CO_2 exposure. However, results from infrared spectroscopy given in the Supporting Information show that, although pure isooctane and reverse micelle solutions do absorb modest levels of CO_2, the aqueous solutions absorb 10 times more CO_2 than isooctane and reverse micellular solutions. The ability of the solutions to absorb CO_2 gas, and most likely other gases, is strongly impacted by the presence or absence of other gases in the solution.

In our experiments, complete acidification of water in reverse micelles by less than *1* atm of CO_2 occurred in <20 min for all samples measured; reverse micellar samples reached equilibrium in <5 min, much more quickly than bulk aqueous solutions (Figure 6). Our studies convincingly demonstrate that *modest* exposure to CO_2 gas, <1 atm, rapidly and effectively acidifies water pools in AOT reverse micelles. Acidification occurs equally effectively whether gas is added actively by bubbling or passively by displacing air above the sample with CO_2.

B. Polyoxovandate Probes as Intramicellar pH Probes. The results presented here enlist polyoxovanadate chemistry to probe the pH of the intramicellar water pool. Like all molecular probes, vanadate has advantages and limitations.[41] One tremendous advantage is the fact that both the NMR peak positions and vanadate speciation report on the solution pH. Additionally, the range of oxovanadate speciation and protonation states make it possible to probe from highly acidic (pH ~1) to very basic (pH >12) solution using a single probe system.[41,43,44] The range of species and their pK_a values also makes the oxovanadate chemistry particularly effective for exploring small acid/base changes at virtually any pH value. Like some other reports in the literature,[32,37,38] our studies of intramicellar pH indicate that the reverse micelle environment appears to buffer the interior. Unlike the results from Hasegawa,[32] which indicated that the reverse micelles had acidic interiors, the reverse micelles we have measured, AOT (anionic) and Igepal CO-520 (nonionic), buffer the interior toward neutral pH.[15,22,48]

One limitation of the vanadate probe arises from its buffering capacity that leads aqueous vanadate solutions to absorb more CO_2 than aqueous solutions without vanadate.[58,59] Regardless of vanadate concentration, we observe that solutions exposed to CO_2 gas reach similar final pH values, which shows that vanadate does not significantly enhance acidification by CO_2. Because the presence of vanadate does not significantly alter the final pH observed in bulk aqueous solutions, we measure the same intrinsic pH for aqueous solution and in the reverse micelles even though the vanadate-containing solutions absorb more CO_2 than solutions lacking vanadate. Also, the final speciation and hence pH of the reverse micellar water pools are the same whether CO_2 is exposed to the aqueous solution before introducing to the reverse micelles or if the reverse micelles are exposed to CO_2 directly (Figure 5). These studies demonstrating the same acidification by atmospheric CO_2 in both aqueous and reverse micellar solutions are in contrast with studies exposing reverse micelles to high-pressure CO_2, where less acidification occurs in the reverse micelles than in bulk aqueous solution.[54]

We attribute the species formed in the reverse micelles to known oxovanadate species; however, alternative interpretations could exist for the observed data. For example, the vanadium probes could form complexes with carbonate or CO_2. Although some literature reports are available on vanadium complexes with CO_2 or CO_3^{2-}, they refer primarily to vanadium in lower oxidation states or relate to solid-state studies of minerals.[41,43,44,58,59] Because carboxylate complexes with vanadates have spectral signatures significantly different from oxovanadates[41] combined with the low stability of vanadium−carbonate complexes,[58,59] it is unlikely that these species account for our results. Furthermore, the signal positions for probes in aqueous solution and reverse micelles are well-known;[15,22,41] significant perturbation to these probes would change the chemical shifts of the NMR signals. We also considered the possibility that the observed changes in the probe composition could reflect factors other than pH. However, these variables, e.g., ionic strength, temperature, and probe concentration, impact the speciation, as observed by ^{51}V NMR spectroscopy, significantly less than pH.[44] The dramatic changes we observe exceed those associated with effects other than pH changes, leading to the conclusion that the spectral changes result primarily from changing pH in the reverse micelle interiors.

Because we measure the pH change in the reverse micelles with a probe, we cannot confirm unequivocally the pH inside reverse micelles containing only water. IR spectra confirm the absorption of CO_2 by reverse micelle solutions but do not demonstrate intramicellar pH. Measurements designed to

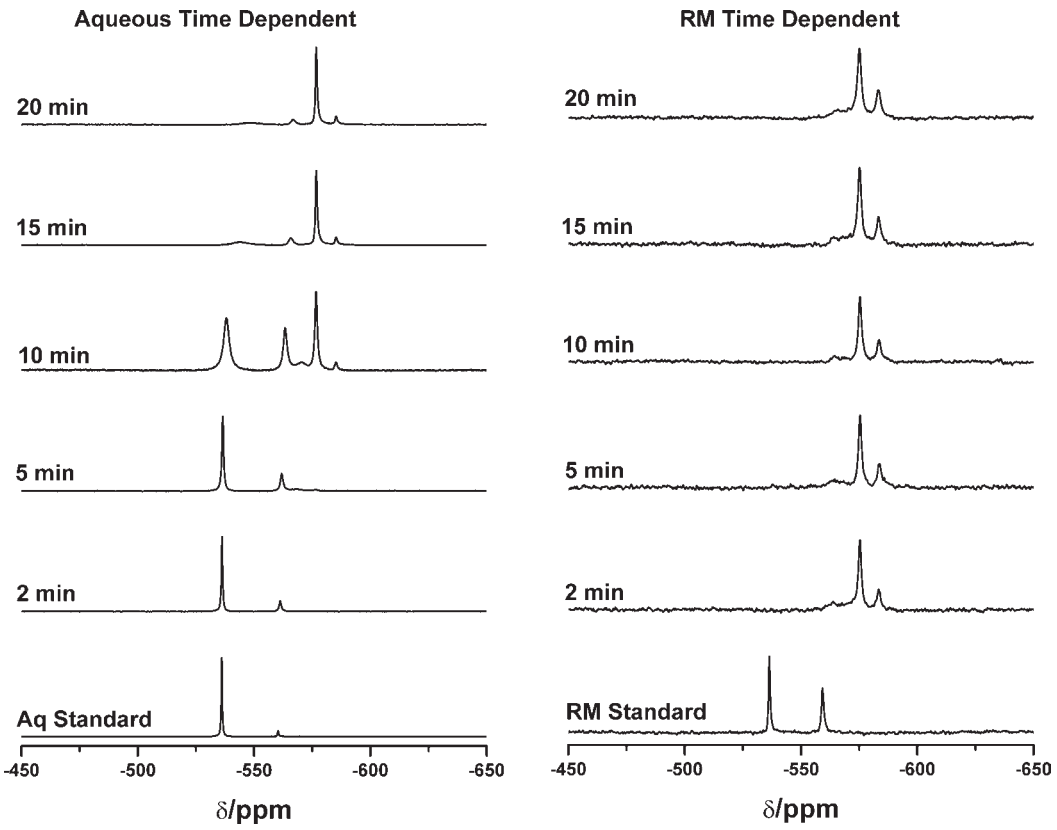

Figure 6. ^{51}V NMR spectra at 78.9 MHz of w_0 = 12 reverse micelle samples in isooctane and aqueous solutions from which samples were formed as a function of time that the samples were exposed to CO_2 gas: (left) aqueous 50 mM $NaVO_3$ prepared to pH 12.00; (right) w_0 = 12 AOT/isooctane reverse micelles formed with 50 mM $NaVO_3$ prepared to pH 12.00. Each spectrum reflects exposure to CO_2 for the indicated amount of time: that is, 2, 5, 10, 15, or 20 min. Aliquots of solution were removed at the times noted, and NMR spectra were collected.

quantitatively measure CO_2 absorption by the reverse micelle solutions both with and without vanadate yielded results indistinguishable from those for pure isooctane, demonstrating that the vanadate-containing reverse micelles do not absorb significantly more compared to non-vanadate-containing reverse micelles. Taken together with the insensitivity to reverse micelle size and to the order of exposure, we believe that our results reflect the drop in pH that would be observed if we could measure the acidity without the vanadate probe. A recent application[40] measuring acidity inside reverse micelles using NMR relaxation (T_2) could potentially detect reverse micelle acidification by CO_2, and we plan to explore this method to detect CO_2 acidification in AOT reverse micelles with and without the vanadate probes.

C. Quantitative Considerations of CO_2 (g) Absorption in Reverse Micelles. Through changes in the vanadate speciation, we observe the overall reaction of CO_2 gas conversion to aqueous H^+ and HCO_3^- (eq 2) rather than each step of the reaction in eq 1. The chemical potential gradient causes absorption, diffusion and subsequent reaction of the CO_2 in solution. The observed changes in vanadate species upon exposure to CO_2 indicate significant production of protons in the vanadate environment. Conversion of CO_2 gas to H^+ (aq) and HCO_3^- (aq) generates the protons responsible for the changes in vanadate speciation. The equilibrium speciation, that is, the vanadate oligomers observed at the end of the reaction in aqueous solution are experimentally indistinguishable from those observed in the reverse micelles and indicates the overall reaction equilibrium does not shift significantly in the confined environment.

$$H_2O(l) + CO_2(g) \overset{K_a'}{\rightleftharpoons} H^+(aq) + HCO_3^-(aq) \qquad (2)$$

For bulk aqueous solution, we can measure the equilibrium constant and hence the pK_a' value for the reaction given in eq 2 by knowing the pressure of CO_2 gas and the concentrations of H^+(aq) and HCO_3^-(aq). The pressure of the CO_2 is 0.84 atm; using $c = P/RT$ with T = 300 K, we find the contribution from CO_2(g) is 3.4 × 10^{-2} M. For aqueous solutions, [H^+] is given by the final pH 6.5; therefore, [H^+] = $10^{-6.5}$ M = 3.2 × 10^{-7} M. The concentration of bicarbonate is equal to the sum of the concentration of [H^+] present in the solution at equilibrium, 3.2 × 10^{-7} M, plus the concentration of protons consumed to produce the vanadate oligomers and the concentration of protons required to lower the pH from 11.8 to 6.5, 6.2 mM. The number of protons consumed by vanadate in the speciation change is equal to the number of vanadium atoms, 50 mM. The overall [HCO_3^-] = [$NaVO_3$] = 50 mM. These values yield pK_a' = 6.3, very near the literature value of 6.35.[4−6]

Deriving a value for the pK_a' value in the reverse micelles presents a significant challenge, because we do not have effective methods to evaluate, or even understand in some cases, the relevant concentration values. Assuming the local concentration in the reverse micelles is the same as the solutions from which samples are prepared yields the identical pK_a' = 6.3 as for bulk aqueous solution. Alternatively, we can use the overall concentration of

Scheme 1. Equilibrium Present at pH 11.8 (Reaction 1) and Major Reactions Occurring upon a pH Drop from 11.8 to 6.5 (Reactions 2−5)

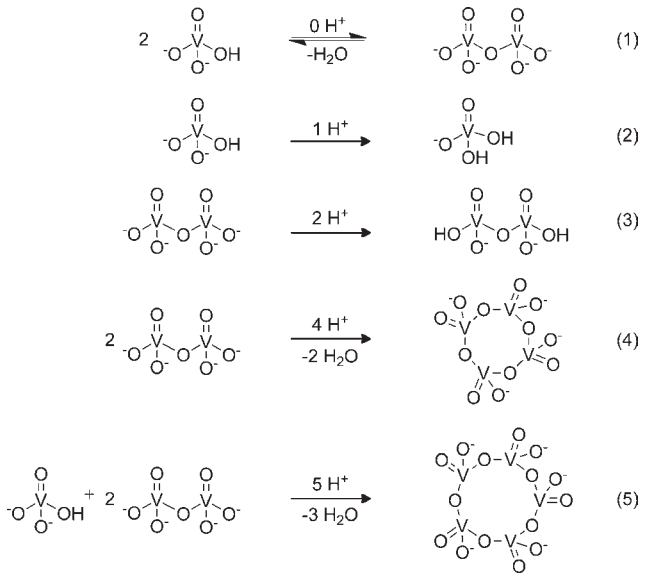

species in solution to estimate the pK_a' of the reaction given in eq 2. In this case, $[CO_2(g)]$ is assumed to remain the same as it is for the bulk aqueous solution, 3.4×10^{-2} M. To obtain values for $[H^+]$ and $[HCO_3^-]$, we must dilute by the relative amount of aqueous solution added to the overall solution. This yields $[HCO_3^-] = 2.4 \times 10^{-3}$ M and $[H^+] = 1.4 \times 10^{-11}$, resulting in $K_a' = 9.9 \times 10^{-13}$. Clearly, this value is so minuscule as to have no effect on the pH of the solution. However, the vanadium probes indicate that the environment inside the reverse micelles has a pH value similar to that found in aqueous solution.

Other considerations to obtain values for $[H^+]$ and $[HCO_3^-]$ are based on the local concentration of species, calculating the $H^+(aq)$ and $HCO_3^-(aq)$ concentrations by estimating the volume taken by the aqueous solution in the reverse micelles and estimating the number of solutes, H^+, oxovanadates, and HCO_3^-, in individual reverse micelles. With 1553 water molecules in each reverse micelle, we calculate the water pool volume assuming that the water is 55 M, $V_{rm} = 4.7 \times 10^{-23}$ L. The presence of one solute molecule in this water pool leads to a concentration of 35 mM. At a lower limit, one H^+ and one HCO_3^- reside in the water pool. Assuming the same exposure to $CO_2(g)$, we obtain $K_a' = 3.6 \times 10^{-2}$ or $pK_a' = 1.4$.

Generating 1.5−2 H^+ ions per reverse micelle that we observe through CO_2 absorption requires an enormous amount of the gas-phase molecule; each reverse micelle would have to absorb millions or more CO_2 molecules to achieve conversion of $CO_2(g)$ to $H^+(aq)$ and $HCO_3^-(aq)$. Although vanadate causes more CO_2 to be absorbed, in the absence of the vanadate chemistry, the reverse micelles still absorb an unrealistically large amount of CO_2. This type of rationale demonstrates the problem with applying equations derived for macroscopic systems to the nanoscopic environment in a reverse micelle with only ~1500 water molecules.[13,24] Although the conventional definition of pH breaks down in the confined environment, the nanoscopic water pools respond to acidification, granting the ability to compare bulk phenomena to that in nonconventional media. Importantly, the vanadium probes allow us to measure acid−base properties within the water pools, regardless of how we define acidity.

The microheterogeneous nature of reverse micellar samples supports reactions more complex than in aqueous solution. If the reaction rates were identical in the reverse micelles and in aqueous solution, it might seem reasonable with 20 times less vanadate reactant that the reaction reaches equilibrium faster, as shown in Figure 6. Twice as much CO_2 dissolves in isooctane than in a comparable volume of water, which may facilitate CO_2 absorption into the reverse micelle water pools. IR spectra of reverse micelle samples exposed to CO_2 reveal its presence in the nonpolar environment of the microemulsions. In aqueous solution, $CO_2(g)$ is absorbed and generates H^+, as shown in eq 1, and the vanadium probes in solution respond by well-understood oligomerization and protonation reactions. Each reverse micelle contains on average 1.5 vanadium atoms; thus, the same speciation changes require not only absorption of $CO_2(g)$ and its conversion to the acid but also collisions among the reverse micelles supplying the necessary number of vanadium atoms to form the observed oligomers. Because the diffusion coefficient for reverse micelles through solution is ~20 times smaller than that for CO_2 through water, we expect the relative rate of reaction to be slower for the complex reverse micelle samples compared to that for bulk aqueous solution. However, the vanadate speciation reactions reach equilibrium at least four times faster in the reverse micelles than in bulk aqueous solution, suggesting that the overall reaction is faster in the reverse micellar environment.

Our observation that the overall reaction, eq 2, is faster in the reverse micelles than in bulk aqueous solution may suggest that we generate H_2CO_3 faster in reverse micelles than it is produced in aqueous solution. Using ultrafast IR spectroscopy, Adamczyk et al.[60] reported direct observation of H_2CO_3 conversion to H^+ and HCO_3^- in bulk aqueous solution with a pK_a of 3.45, which is consistent with literature data.[4−6] Results presented here suggest that H_2CO_3 should persist long enough to be observed directly through ultrafast infrared spectroscopy experiments in reverse micellar media. Combining these studies provides tools for studies involving CO_2 and H_2CO_3 in nanodroplets in the future.

V. CONCLUSION

The results reported here have significant implications for absorption of CO_2 and other atmospheric gas-phase molecules into droplets in microheterogeneous media. Although researchers have demonstrated acidification in reverse micelles under extreme conditions of high pressure and supercritical CO_2,[54−56] we are unaware of studies exploring the effect of ambient-pressure and -temperature CO_2 on reverse micelles. The data we present in our paper represent the first of their kind, demonstrating acidification of the reverse micelle water pools by *ambient*-pressure and -temperature gaseous CO_2.

Although it is more difficult to detect, we have observed atmospheric carbon dioxide (pCO_2 ~370 ppm[61]) acidify the water in reverse micelles equilibrated with atmospheric gases. We have also observed prompt acidification by degassed samples. These results demonstrate the permeability of the reverse micelles to molecular gases extending from CO_2 to O_2, NO, and others. The effects of ambient CO_2 on water in nanoscale environments have largely been ignored, potentially because of the small equilibrium constant in aqueous solution for the formation of carbonic acid from $CO_2(g)$.[4−6] Invoked as models for aerosol droplets[12] and as nanoreactors,[9] the demonstration of

CO_2 absorption into reverse micelles has implications for the acidities of nanoscopic water pools in a range of applications. The fact that CO_2 is absorbed in these nanosized water droplets documents an as of yet unrecognized but important role of atmospheric CO_2 in these systems.

■ ASSOCIATED CONTENT

Supporting Information. Text, a scheme, and a table giving detailed information about calculations performed to estimate the number of protons necessary for the vanadate speciation changes observed and details about infrared spectroscopy measurements. This material is available free of charge via the Internet at http://pubs.acs.org.

■ AUTHOR INFORMATION

Corresponding Author

*E-mail: Nancy.Levinger@ColoState.edu; Debbie.Crans@ColoState.edu.

Present Addresses

†Department of Chemistry and Biochemistry, Kennesaw State University, Kennesaw, GA 30144.

■ ACKNOWLEDGMENT

This material is based upon work supported by the National Science Foundation under Grant 0628260 (CRC). L.C.R. gratefully acknowledges support from the NSF REU program at Colorado State University (NSF 0649263) and the CSU Undergraduate Research Institute, funded in part by a grant from the Research Corp. We acknowledge Ms. J. Alcock, who performed preliminary experiments on these systems, Prof. S. H. Strauss, Mr. D. L. Heyliger, Mr. T. Folsom, and Dr. P. Chatterjee for quantitative measures of CO_2 absorption, Prof. E. R. Fisher for access to FTIR, and fruitful discussions with Dr. E. Gaidamauskus, Dr. C. R. Roberts, and Prof. B. L. Gourley.

■ REFERENCES

(1) Cox, P. M.; Betts, R. A.; Jones, C. D.; Spall, S. A.; Totterdell, I. J. *Nature* **2000**, *408*, 184–187.
(2) Feely, R. A.; Sabine, C. L.; Hernandez-Ayon, J. M.; Ianson, D.; Hales, B. *Science* **2008**, *320*, 1490–1492.
(3) Roos, A.; Boron, W. F. *Physiol. Rev.* **1981**, *61*, 296–434.
(4) Gibbons, B. H.; Edsall, J. T. *J. Biol. Chem.* **1963**, *238*, 3502–3507.
(5) Ho, C.; Sturtevant, J. M. *J. Biol. Chem.* **1963**, *238*, 3499–3501.
(6) Wissbrun, K. F.; French, D. M.; Patterson, A. *J. Phys. Chem.* **1954**, *58*, 693–695.
(7) Mucha, M.; Frigato, T.; Levering, L. M.; Allen, H. C.; Tobias, D. J.; Dang, L. X.; Jungwirth, P. *J. Phys. Chem. B* **2005**, *109*, 7617–7623.
(8) Subir, M.; Liu, J.; Eisenthal, K. B. *J. Phys. Chem. C* **2008**, *112*, 15809–15812.
(9) Cushing, B. L.; Kolesnichenko, V. L.; O'Connor, C. J. *Chem. Rev.* **2004**, *104*, 3893–3946.
(10) Luisi, P. L.; Giomini, M.; Pileni, M. P.; Robinson, B. H. *Biochim. Biophys. Acta* **1988**, *947*, 209–246.
(11) Hoffmann, M. M.; Heitz, M. P.; Carr, J. B.; Tubbs, J. D. *J. Dispersion Sci. Technol.* **2003**, *24*, 155–171.
(12) Dobson, C. M.; Ellison, G. B.; Tuck, A. F.; Vaida, V. *Proc. Natl. Acad. Sci. U.S.A.* **2000**, *97*, 11864–11868.
(13) De, T.; Maitra, A. *Adv. Colloid Interface Sci.* **1995**, *59*, 95–193.
(14) Chakrabarty, D.; Seth, D.; Chakraborty, A.; Sarkar, N. *J. Phys. Chem. B* **2005**, *109*, 5753–5758.
(15) Baruah, B.; Roden, J.; Sedgwick, M.; Correa, N. M.; Crans, D. C.; Levinger, N. E. *J. Am. Chem. Soc.* **2006**, *128*, 12758–12765.
(16) Piletic, I. R.; Moilanen, D. E.; Spry, D. B.; Levinger, N. E.; Fayer, M. D. *J. Phys. Chem. A* **2006**, *110*, 4985–4999.
(17) Riter, R. E.; Willard, D. M.; Levinger, N. E. *J. Phys. Chem. B* **1998**, *102*, 2705–2714.
(18) Faeder, J.; Ladanyi, B. M. *J. Phys. Chem. B* **2000**, *104*, 1033–1046.
(19) Mugridge, J. S.; Szigethy, G.; Bergman, R. G.; Raymond, K. N. *J. Am. Chem. Soc.* **2010**, *132*, 16256–16264.
(20) Rodriguez, J.; Laria, D.; Guardia, E.; Marti, J. *Phys. Chem. Chem. Phys.* **2009**, *11*, 1484–1490.
(21) Levinger, N. E.; Swafford, L. A. *Annu. Rev. Phys. Chem.* **2009**, *60*, 385–406.
(22) Baruah, B.; Crans, D. C.; Levinger, N. E. *Langmuir* **2007**, *23*, 6510–6518.
(23) Holmes, J. D.; Ziegler, K. J.; Audriani, M.; Lee, C. T.; Bhargava, P. A.; Steytler, D. C.; Johnston, K. P. *J. Phys. Chem. B* **1999**, *103*, 5703–5711.
(24) Chowdhury, P. K.; Ashby, K. D.; Datta, A.; Petrich, J. W. *Photochem. Photobiol.* **2000**, *72*, 612–618.
(25) Moilanen, D. E.; Fenn, E. E.; Lin, Y. S.; Skinner, J. L.; Bagchi, B.; Fayer, M. D. *Proc. Natl. Acad. Sci. U.S.A.* **2008**, *105*, 5295–5300.
(26) Moilanen, D. E.; Fenn, E. E.; Wong, D.; Fayer, M. D. *J. Chem. Phys.* **2009**, *131*, 014704.
(27) Crans, D. C.; Trujillo, A. M.; Bonetti, S.; Rithner, C. D.; Baruah, B.; Levinger, N. E. *J. Org. Chem.* **2008**, *73*, 9633–9640.
(28) Chen, J.; Zhang, J. L.; Han, B. X.; Feng, X. Y.; Hou, M. Q.; Li, W. J.; Zhang, Z. F. *Chem. Eur. J.* **2006**, *12*, 8067–8074.
(29) Zhang, J. S.; Lee, S.; Lee, J. W. *J. Chem. Eng. Data* **2008**, *53*, 1321–1324.
(30) Rodriguez, J.; Marti, J.; Guardia, E.; Laria, D. *J. Phys. Chem. B* **2007**, *111*, 4432–4439.
(31) Silber, J. J.; Biasutti, A.; Abuin, E.; Lissi, E. *Adv. Colloid Interface Sci.* **1999**, *82*, 189–252.
(32) Hasegawa, M. *Langmuir* **2001**, *17*, 1426–1431.
(33) Falcone, R. D.; Correa, N. M.; Biasutti, M. A.; Silber, J. J. *J. Colloid Interface Sci.* **2006**, *296*, 356–364.
(34) Falcone, R. D.; Correa, N. M.; Biasutti, M. A.; Silber, J. J. *Langmuir* **2002**, *18*, 2039–2047.
(35) Liao, K. L.; Xu, X. Z.; Du, X. Z. *J. Colloid Interface Sci.* **2010**, *341*, 280–285.
(36) Oshitani, J.; Takashina, S.; Yoshida, M.; Gotoh, K. *J. Chem. Eng. Jpn.* **2008**, *41*, 507–512.
(37) Mchedlov-Petrossyan, N. O.; Vodolazkaya, N. A.; Gurina, Y. A.; Sun, W.-C.; Gee, K. R. *J. Phys. Chem. B* **2010**, *114*, 4551–4564.
(38) Vodolazkaya, N. A.; McHedlov-Petrossyan, N. O.; Salamanova, N. V.; Surov, Y. N.; Doroshenko, A. O. *J. Mol. Liq.* **2010**, *157*, 105–112.
(39) Zhao, Y. J.; Zhang, J. L.; Han, B. X.; Zhang, C. X.; Li, W.; Feng, X. Y.; Hou, M. Q.; Yang, G. Y. *Langmuir* **2008**, *24*, 9328–9333.
(40) Halliday, N. A.; Peet, A. C.; Britton, M. M. *J. Phys. Chem. B* **2010**, *114*, 13745–13751.
(41) Crans, D. C.; Smee, J.; Gaidamauskas, E.; Yang, L. *Chem. Rev.* **2004**, *104*, 849–902.
(42) Pope, M. T.; Muller, A. *Angew. Chem., Int. Ed. Engl.* **1991**, *30*, 34–48.
(43) Pettersson, L.; Hedman, B.; Anderson, I. *Chem. Scr.* **1983**, *60*, 254–264.
(44) Tracey, A. S.; Jaswal, J. S.; Angusdunne, S. J. *Inorg. Chem.* **1995**, *34*, 5680–5685.
(45) Because the gaseous CO_2 is introduced to the sample via sublimed dry ice and the studies were performed at high altitude, the CO_2 pressure is 0.84 atm, the average atmospheric pressure in Fort Collins, CO, where this study was conducted.
(46) Stahla, M. L.; Baruah, B.; James, D. M.; Johnson, M. D.; Levinger, N. E.; Crans, D. C. *Langmuir* **2008**, *24*, 6027–6035.
(47) Crans, D. C.; Rithner, C. D.; Baruah, B.; Gourley, B. L.; Levinger, N. E. *J. Am. Chem. Soc.* **2006**, *128*, 4437–4445.

(48) Sedgwick, M. A.; Crans, D. C.; Levinger, N. E. *Langmuir* **2009**, *25*, 5496–5503.
(49) Li, Q.; Li, T.; Wu, J. *J. Colloid Interface Sci.* **2001**, *239*, 522–527.
(50) Sih, R.; Dehghani, F.; Foster, N. R. *J. Supercrit. Fluids* **2007**, *41*, 148–157.
(51) Kinugasa, T.; Kondo, A.; Nishimura, S.; Miyauchi, Y.; Nishii, Y.; Watanabe, K.; Takeuchi, H. *Colloid Surf. A* **2002**, *204*, 193–199.
(52) Jacobson, G. B.; Lee, C. T.; Johnston, K. P. *J. Org. Chem.* **1999**, *64*, 1201–1206.
(53) Ji, M.; Chen, X. Y.; Wai, C. M.; Fulton, J. L. *J. Am. Chem. Soc.* **1999**, *121*, 2631–2632.
(54) Liu, D. X.; Zhang, J. L.; Han, B. X.; Fan, J. F.; Mu, T. C.; Liu, Z. M.; Wu, W. Z.; Chen, J. *J. Chem. Phys.* **2003**, *119*, 4873–4878.
(55) Shen, D.; Buxing, H.; Dong, Y.; Chen, J.; Tiancheng, M.; Weize, W.; Zhang, J. *J. Phys. Chem. B* **2005**, *109*, 5796–5801.
(56) Niemeyer, E. D.; Bright, F. V. *J. Phys. Chem. B* **1998**, *102*, 1474–1478.
(57) Wilcock, R. J.; Battino, R.; Danforth, W. F.; Wilhelm, E. *J. Chem. Thermodyn.* **1978**, *10*, 817–822.
(58) Crans, D. C. *Met. Ions Biol. Syst.* 1995, *31*, 147–209.
(59) Meier, R.; Werner, G.; Kirmse, R.; Stach, J.; Dunsch, L. *Z. Anorg. Allg. Chem.* **1990**, *583*, 209–222.
(60) Adamczyk, K.; Premont-Schwarz, M.; Pines, D.; Pines, E.; Nibbering, E. T. J. *Science* **2009**, *326*, 1690–1694.
(61) Boniface, J.; Shi, Q.; Li, Y. Q.; Cheung, J. L.; Rattigan, O. V.; Davidovits, P.; Worsnop, D. R.; Jayne, J. T.; Kolb, C. E. *J. Phys. Chem. A* **2000**, *104*, 7502–7510.